APPLICATIONS PAPER

High Resolution Imagery Collection for Post-Disaster Studies Utilizing Unmanned Aircraft Systems (UAS)

Stuart M. Adams, Marc L. Levitan, and Carol J. Friedland

Abstract

This paper examines the use of unmanned aircraft systems (UAS) to capture imagery for use in post-disaster field studies at the neighborhood and individual building level. A discussion of post-disaster imagery collection including satellite, aerial, and ground-based platforms is first presented. Applications of UAS in recent disasters as described in the literature are then surveyed, and a case study investigating UAS capabilities for imagery collection following an EF-3 tornado in northern Alabama on 02 March 2012 is presented. Case study considerations include the multi-rotor unmanned aerial vehicle (UAV) equipment and ground station, onboard imagery devices, flight considerations and capabilities, and imagery and metadata collection capabilities of the UAS. Sample post-tornado imagery of building damage is shown, demonstrating the order of magnitude improvement in imagery resolution compared to traditional post-disaster aerial photography.

Introduction

Damage assessments following disaster events are often performed using imagery acquired through satellite, aerial, and ground-based (vehicle-mounted and handheld) platforms, which can be analyzed using visual, spectral, and photogrammetric techniques. Satellite and aerial imagery covers large geographical areas but are of limited use for detailed investigations of individual buildings and neighborhoods due to spatial resolution limitations. Additionally, while such imagery is usually available following large disasters such as the Joplin, Missouri, tornado in 2011 and Hurricane Sandy in 2012, it may not be readily available following smaller events.

Imagery for use in studies of the performance of the built environment at individual building and neighborhood levels has mainly been obtained by handheld and, more recently, vehicle-mounted cameras. A significant limitation of vehicle-mounted systems is that they are best at collecting images of the street facing side(s) of the building. Side views may or may not be available depending on proximity of adjacent buildings, and views of the rear face of the building are generally not available unless the neighborhoods have alleys. Trees, shrubs, and fences create interference for vehicle-mounted cameras. These elements can also create interference for handheld cameras, but to a lesser extent than the aforementioned obstacles since the photographer has more flexibility in selecting a vantage point. When access to a damaged building is possible, handheld cameras are often used to acquire imagery inside the building and from the roof of the building, to obtain a much fuller understanding of the damage. Imagery collected from the roof, especially roofs of taller buildings, can show damage to adjacent buildings as well. However, in some instances, buildings are too damaged to enter safely. Ground-based imagery acquisition (both handheld and vehicle-based) can be hindered by site access limitations, including: downed trees, power lines, and other debris blocking the roads; roads washed out by storm surge or inland flooding; law enforcement roadblocks; private property and privacy considerations; and physical security considerations for the ground-based damage survey team.

The limitations of existing satellite, aerial, and ground-based imagery platforms also create difficulties when assessing building damage caused by different hazards. For example, storm surge damage to the walls and interior of a building in cases where the roof remained intact may not be visible from nadir (vertical) satellite and aerial imagery. Earthquake-induced collapses where the roof remains largely intact may similarly be difficult to identify from nadir imagery (Gerke and Kerle, 2011). Wind damage to flat or low slope roofs may not be observable from ground based imagery. Additional information on capabilities and limitations of the different imagery platforms are discussed by Adams *et al.* (2010).

Recent advances in UAS flight and flight control capabilities and in digital camera technologies, coupled with substantial reductions in the costs of both, have positioned UAS as platforms of interest for post-disaster studies. UAS provide a user-controlled means to collect imagery from multiple angles at neighborhood and individual building scales. UAV-mounted camera systems have the capability to capture still and video imagery from vertical and oblique perspectives at much higher resolutions than currently available from commercial satellite and aerial photography (Nebiker *et al.*, 2008). UAS also have capabilities to overcome common site access and image collection limitations of ground-based platforms. UAS platforms can thus potentially fill a significant gap in current imagery collection methods for use in assessing and

Stuart M. Adams is with the Department of Civil and Environmental Engineering, Louisiana State University, 3418 Patrick F. Taylor Hall, Baton Rouge, LA 70803 (sadam15@lsu.edu).

Marc L. Levitan is with the National Windstorm Impact Reduction Program, Engineering Laboratory, National Institute of Standards and Technology, 100 Bureau Drive, Gaithersburg, MD, 20899 (marc.levitan@nist.gov).

Carol J. Friedland is with Bert S. Turner Department of Construction Management, Louisiana State University, 3128 Patrick F. Taylor Hall, Baton Rouge, LA 70803 (friedland@lsu.edu).

Photogrammetric Engineering & Remote Sensing
Vol. 80, No. 12, December 2014, pp. 1161–1168.
0099-1112/14/8012–1161

doi: 10.14358/PERS.80.12.1161

evaluating the performance of individual buildings and neighborhoods following disasters.

This paper provides a literature survey of UAS usage for disaster imagery collection and presents a case study investigating UAS capabilities for imagery collection following a strong tornado that struck northern Alabama in March 2012.

Use of Unmanned Aircraft Systems for Post-Disaster Imagery Collection

Use of unmanned aircraft systems for data collection has been reported following hurricane and typhoon, earthquake, tsunami, fire, and landside disasters. UAS have also been used following structural collapses, e.g., a miniature helicopter UAS was used in the 2007 parking garage failure investigation in Jacksonville, Florida (Murphy, 2012).

Post-hurricane uses reported in the literature include structural damage inspections for several multi-story commercial buildings impacted by Hurricane Katrina (Pratt *et al.*, 2006) and inspections of seawalls and piers damaged by Hurricane Wilma (Steimle *et al.*, 2009). For the Hurricane Katrina inspections, two small unmanned aircraft systems (sUAS) were deployed to take high-resolution optical and thermal imagery. A Like90 T-Rex helicopter provided imagery from distances as far as 76 m and as close as 2 to 5 m away from the building envelope. Additionally, a 1.2 m long fixed-wing sUAS equipped with optical and thermal imagery devices provided imagery from 30 to 300 m. A point-of-view camera was also included on the fixed-wing sUAV for pilot navigation purposes. Three operators including a pilot, flight director, and mission specialist were present during the assessment operations. The Hurricane Wilma assessments utilized an iSENSYS rotary-wing, sUAS, equipped with a visible-light camera which transmitted imagery to a camcorder for real-time visualization and recording purposes. The UAS had an allowable wind tolerance of 15 m/s and was operated by a pilot and mission specialist.

UAS have also been deployed for post-disaster earthquake imagery collection in L'Aquila, Italy in 2009 and in Haiti in 2010. Following the L'Aquila earthquake, UAVs furnished with cameras were used to inspect buildings and provide tactical information (Quartisch *et al.*, 2010). The L'Aquila earthquake area was also used to explore the application of UAS for fire service response (Murphy, 2011). After the Haiti earthquake, a private company flew a small UAS to assess orphanage damage in remote mountains near Port-au-Prince (Huber, 2011). This propeller-driven UAV was equipped with a camera for long-range video transmission and capable of three hour flight durations with a range of 15 km. The UAV relayed real-time imagery that indicated that the orphanage's critical infrastructure was intact, allowing rescue efforts to concentrate on other areas of need, rather than spending valuable response time to travel to the remote orphanages for reconnaissance (VT Group, 2011).

In March of 2011, Japan endured a devastating earthquake and subsequent tsunami. The Fukushima Daiichi nuclear facility was significantly damaged in the event and consequently began to emit radiation. This hazard complicated traditional reconnaissance efforts as humans were advised to avoid the area. To remedy the imagery collection issue, remotely operated UAS were deployed to the area. A T-Hawk Aerial Vehicle outfitted with special radiation sensors completed five reconnaissance missions of the Fukushima Daiichi plant (Reavis and Hem, 2011). Due to its smaller size and nimble, single rotor flight design, the T-Hawk UAS was able to acquire valuable imagery, including hours of video, at lower altitudes than the Global Hawk, a military-grade UAS that was also deployed to the site (Ackerman, 2011).

Providing imagery reconnaissance for fire monitoring is another documented usage of UAS. An unmanned, fixed-wing, Predator B UAS equipped with infrared imagery sensors was used for fire hot spot detection in San Diego County in October 2007 (Cohen, 2007). Cohen highlighted the inherent safety advantages for pilots and enhanced flight time capabilities (as many as 30 continuous hours) as advantages of the UAS platform, but identified attaining Federal Aviation Administration (FAA) permission for each flight as a significant hurdle to overcome. Other UAS uses include damage assessment in 2009 of the Angeles National Forest by a National Aeronautics and Space Administration (NASA) Predator with infrared imaging capabilities (Fox News, 2013) and real-time imagery transmission from a Predator UAS to help firefighters address a fire in Yosemite National Park (Vincenzi *et al.*, 2014). Vincenzi *et al.* also documents the usage of a small UAS to collect imagery for damage assessment and to provide real-time video to rescue personnel following a landslide near Arlington, Washington, in March 2014.

Case Study: Post-Tornado Reconaissance Using a Small Multi-Rotor UAS

On 02 March 2012, an EF-3 tornado (estimated peak winds as high as 63 m/s) created a damage path over 54 km long near Athens and Harvest, Alabama (NOAA, 2012). Structures along the path suffered significant damage to the building envelope including widespread roof damage. A small remote controlled, multi-rotor UAS capable of manual, semi-autonomous and fully-autonomous flight was deployed for testing as an imagery acquisition platform for post-disaster studies of building damage and performance. The custom-designed UAS, along with a custom ground control station (see Figure 1), was equipped with a digital camera capable of dynamic imagery transmission and remote shutter triggering initiated by the operator. A 12.1 megapixel Panasonic Lumix DMC-TS3 digital camera was mounted to the underside of the UAV and proved to be useful for nadir imagery collection. Additionally, a forward-facing Go Pro Hero 2 HD camera for first-person-viewer (FPV) flight was attached and used for video imagery. In-flight video from the FPV and image capturing cameras was transmitted to the ground control station and used to assist flight control and image quality. The UAV's physical properties included a 0.25 m diameter body, which encased controls, transmitters, and two lithium polymer (lipo) batteries. Three, 0.75 m carbon-fiber arms with 300 W brushless motors mounted at the ends, extended from the UAV body; thus, equating to a total UAV dimension of 1 m in diameter with a maximum height of 0.15 m. The flight weight of the UAV was approximately 3 kg and consisted of a 1.75 kg UAV body and frame with a maximum payload capacity of 1.5 kg. For this study, the payload was 1.275 kg and consisted of two 0.5 kg batteries, a 0.175 kg still camera, and 0.10 kg video camera. The custom UAS (UAV, ground control station, and sensors) cost less than $6,000 USD with the UAV and batteries totaling approximately $1,000 USD, sensors $600 USD, ground control station components $2,500 USD, and an eight-channel external pilot's console $1,000 USD.

The battery-powered custom UAV has a 20 to 30 min flight time depending on payload weight, wind, and flight plan. Wind tolerance of the UAS is below 12 m/s for semi-autonomous and fully-autonomous flights and up to 15 m/s for manually operated flights. The UAS has the ability to fly at speeds up to 12.5 m/s and at an elevation over 500 m above ground level (AGL). The onboard and ground station software include ArduCopter 2.7.3 Mission Planner and ArduPilot Mega. These software platforms enable autonomous stabilization, position hold, waypoint navigation and two way telemetry capabilities.

FAA regulations govern acceptable flight parameters for public entities through a required, individually issued Certificate of Authorization or Waiver (CoA). CoAs define specific airspace available for each public entity's UAS usage, as well

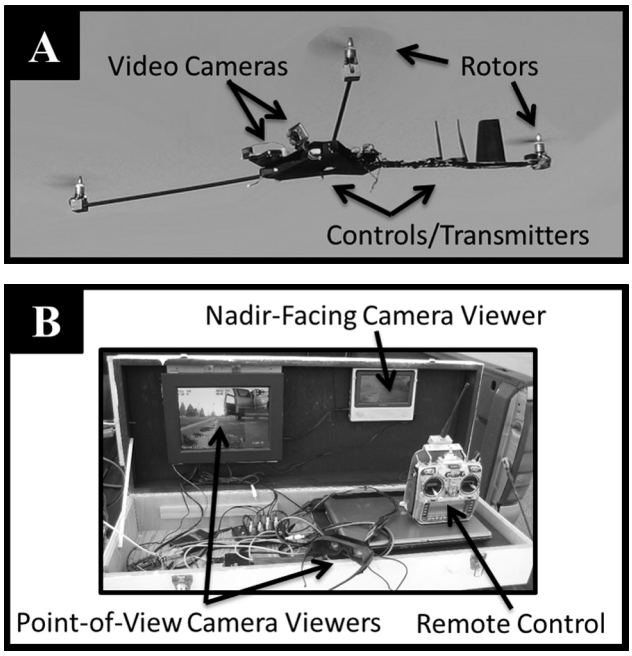

Figure 1. UAS consisting of: (A) Multi-rotor UAV, and (B) Ground Control Station. The UAV is equipped with three rotors, one front-facing video camera, one nadir-facing video camera, and onboard controls and transmitters. The ground control station includes two point-of-view camera viewers (e.g., one display and one wearable, first-person viewer) to aid in flight control and a video camera viewer for instantaneous imagery acquisition review.

as the permissible tasks for airworthy UAS. The airworthiness designation is performed by the public entity, using discretion; however, every UAS's specifications, including lost-link procedures, must be defined in the CoA. Emergency responders with large, yet finite districts (e.g., county sheriff's agency) can apply for a CoA to encompass the entire district; however, a one hour notice to the FAA for usage outside of typical training airspace (as defined in the CoA) should be followed. Emergency responders that address issues in various locations must first receive a CoA that defines a training airspace, and then contact the FAA for permission to use an airworthy UAS in an emergency response capacity outside the CoA-defined, training airspace (FAA outlines a 24-hour timeline for approval). Post-tornado images shown in this paper were collected under FAA hobbyist UAS guidelines requiring line of sight operation and 122 m AGL flight ceilings (FAA, 2011).

For the post-tornado case study, two severely damaged residential buildings were selected as the primary structures to be used in investigating the capabilities of the UAS platform. Figure 2 depicts the flight paths chosen for imagery acquisition. The somewhat erratic nature of the flight paths can be attributed to manual control of the UAV, as semi-autonomous and fully-autonomous flight modes were not pursued due to the high variability and strength of the wind gusts. Flight elevations that enabled the UAV to vertically clear the structures at a comfortable distance, while maintaining operator-to-UAV proximity (preferable in high wind environments) were pursued. Structure 1 was a two-story home with considerable damage to the roof and second story. Ground access to this structure was limited due to a wooden fence (Figure 3A) and the unstable nature of the damaged structure, particularly considering the relatively strong winds occurring at the time of the site visit. The flight path chosen was initiated in an open field nearby and included three ellipsoidal passes of approximately 8 min each at an average flight elevation of 15 m AGL. During the Structure 1 flight, a deviation to investigate a neighboring structure with significant roof damage was made to demonstrate the distance capability of the UAS (Structure 3, approximately 200 m from Structure 1). Figure 3B shows Structure 2, a one-story home with considerable roof damage. Numerous passes during the 20 min flight duration were taken to provide imagery from multiple viewpoints at an average flight elevation of 10 m AGL.

Figures 4, 5, and 6 show a singular image of the house identified as Structure 1, at different zoom levels, collected using the nadir-mounted digital camera on the UAV during the case study. The image was collected at an altitude of approximately 15 m AGL and has a ground sample distance (GSD) of approximately 0.007 m (i.e., distance between centers of adjacent pixels as measured on the ground). Figure 4 clearly shows the debris field surrounding the structure, as well as a severely damaged section of the second-story and roof. A partial floor plan of the structure can be determined as a bedroom, bathroom, and two closets can be identified from this vantage point. Figure 5 provides a zoomed in image of the top left roof corner of the structure. The construction materials used are easily seen; bricks, sheathing, and roofing materials can clearly be identified. Bathroom roofing materials are absent from the image, indicating a removal of the roof structure as opposed to an inward collapse of the roof. Figure 6 shows an even further zoomed-in view of the same damaged area, demonstrating the very high level of detail obtainable with this UAS. Individual bricks are clearly visible. The remains of red chalk lines on the roof sheathing (used during construction for locating ceiling joists for deck nailing) are visible in areas where the roofing felt and shingles have been removed. The roof decking material on this part of the building can clearly be identified as oriented strand board. The level of detail available in this imagery not only provides in-depth information as to building condition, but can also assist with determination of failure mechanisms and sequences. For example, in Figure 6, the face brick from the second story bathroom wall (in the center right of the picture) fell onto roof sheathing and ceiling joists of the adjacent first story roof, indicating that the first story roof damage occurred first.

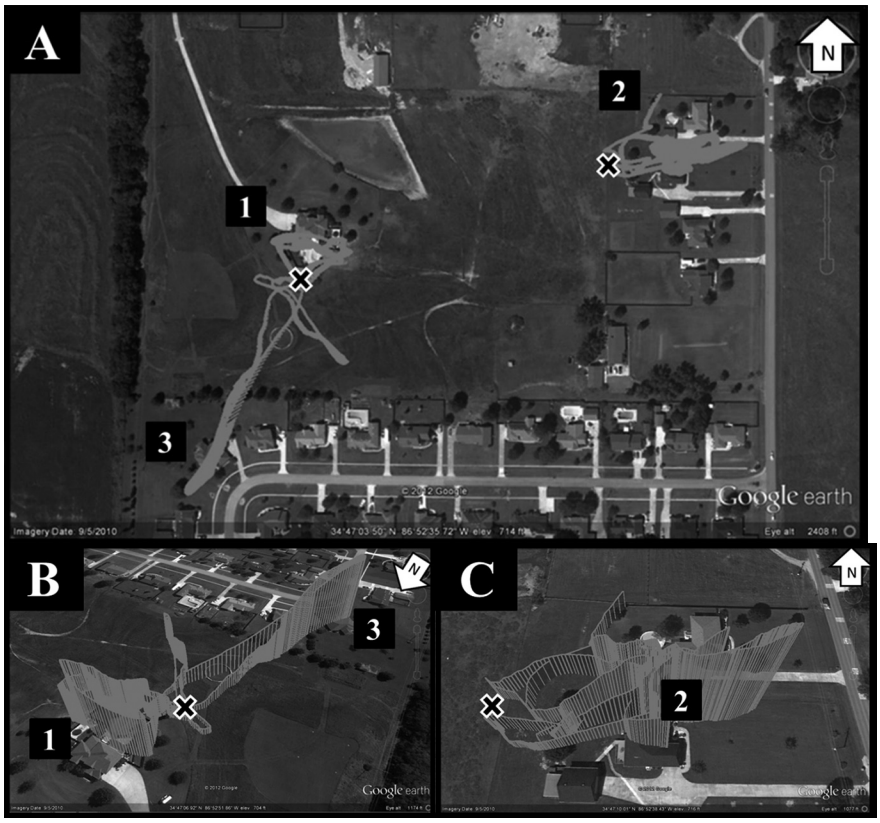

Figure 2. Graphic depicting telemetry data recorded from UAS reconnaissance flights (© Google Earth): (A) Nadir view of flight plan for observing Structures 1 to 3. Isometric views of flight plans for (B) Structures 1 and 3, and (C) Structure 2. Telemetry data including latitude, longitude and altitude above was collected onboard the UAS during flight. Structures 1 and 2 were assessed by multiple UAS passes originating at the locations marked with a black "x."

Figure 3. Ground-based imagery of tornado-damaged structures of interest: (A) southwest facing elevation of Structure 1, a heavily damaged two-story home. The fence and unstable nature of the significantly damaged structure prevented close-range ground-based investigation. (B) West facing elevation of Structure 2, a severely damaged one-story structure. The extent of damage beneath the roof line is difficult to quantify based on this ground-based imagery.

For purposes of comparison, post-disaster National Oceanic and Atmospheric Administration (NOAA) aerial imagery for Hurricane Ike was acquired with an approximate GSD of 0.5 m (NOAA, 2008). Figure 7 (parts A and B) show NOAA aerial images of a residential structure on Galveston. The aerial image seems to show some damage to the roof, although it's difficult to make out specific details. In contrast, the UAS image shown in Figures 4, 5, and 6 has a GSD of approximately 0.007 m, clearly showing damage and allowing identification of specific building materials, such as the usage of oriented strand board (also called OSB) for roof sheathing, as opposed to plywood (the other commonly used residential roof sheathing material). To put it in a different context, a house with 150 m^2 plan view roof area would be represented by approximately 600 pixels on a NOAA aerial image, versus over 3 million pixels on a UAS image with the setup and flight elevation used for Figure 4.

The oblique video frames shown in Figure 8 provide a sense of depth and height of the structure. Watching the video

Figure 4. UAV-based still image of Structure 1 taken by the nadir-mounted digital camera, with GSD approximately 0.007 m.

Figure 5. Close-up image of the southwest corner of the Structure 1, which is from the same image file shown in Figure 5, but shown at a higher zoom. While some roof decking has been removed from the edge, ceiling joists are largely intact for the single story exterior corner room in the top left of the image, while the entire roof and ceiling structure has been removed from the adjacent second floor rooms in the top right of the image.

Figure 6. Further close-up of the southwest corner of Structure 1. This image is from the same imagery files shown in Figures 4 and 5 displayed here at an even higher zoom, which demonstrates the full resolution capabilities of the UAV-mounted camera. Construction materials, and damage to the roof covering, roof sheathing, and ceiling beneath the roof joists are clearly visible.

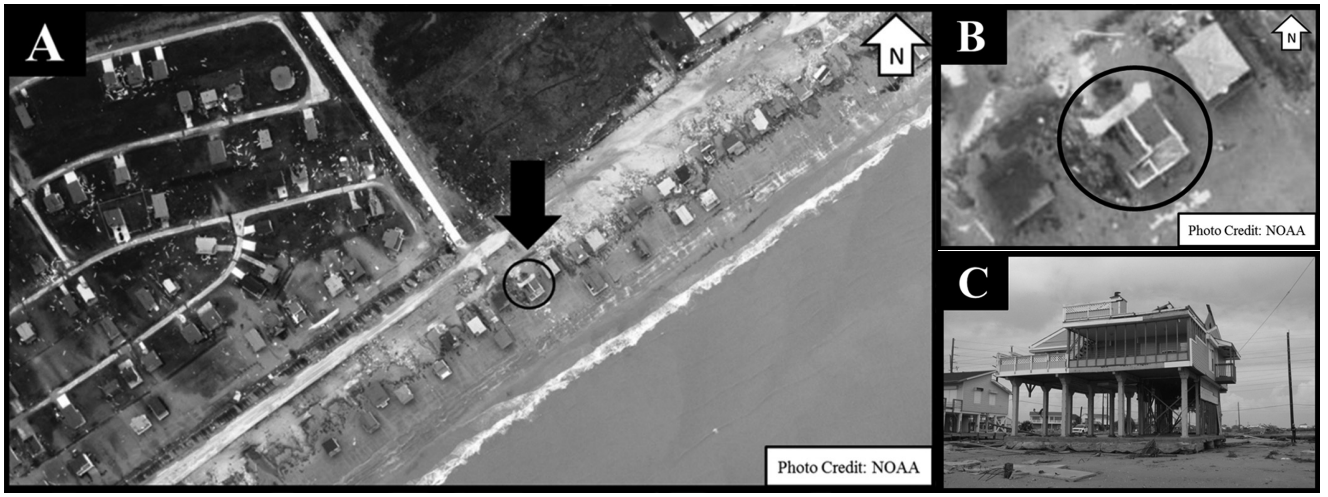

Figure 7. Sample NOAA (2008) post-disaster aerial imagery (NOAA) and ground-based imagery of Galveston, Texas following Hurricane Ike: (A) Neighborhood level NOAA aerial imagery (GSD = 0.5 m) indicates widespread damage to the area through debris fields, and (B) NOAA imagery depicts some type of roof damage as the southwest portion of the roof is discolored; however, the degree of damage is difficult to determine for this multi-level roof and the image provides no information on the façade damage. (C) Ground-based image of the house shown in (B) taken by the lead author. Details of wind damage to the roof are not visible from the ground, and storm surge has destroyed the stairs, so there is no access to enter the structure and investigate from the inside.

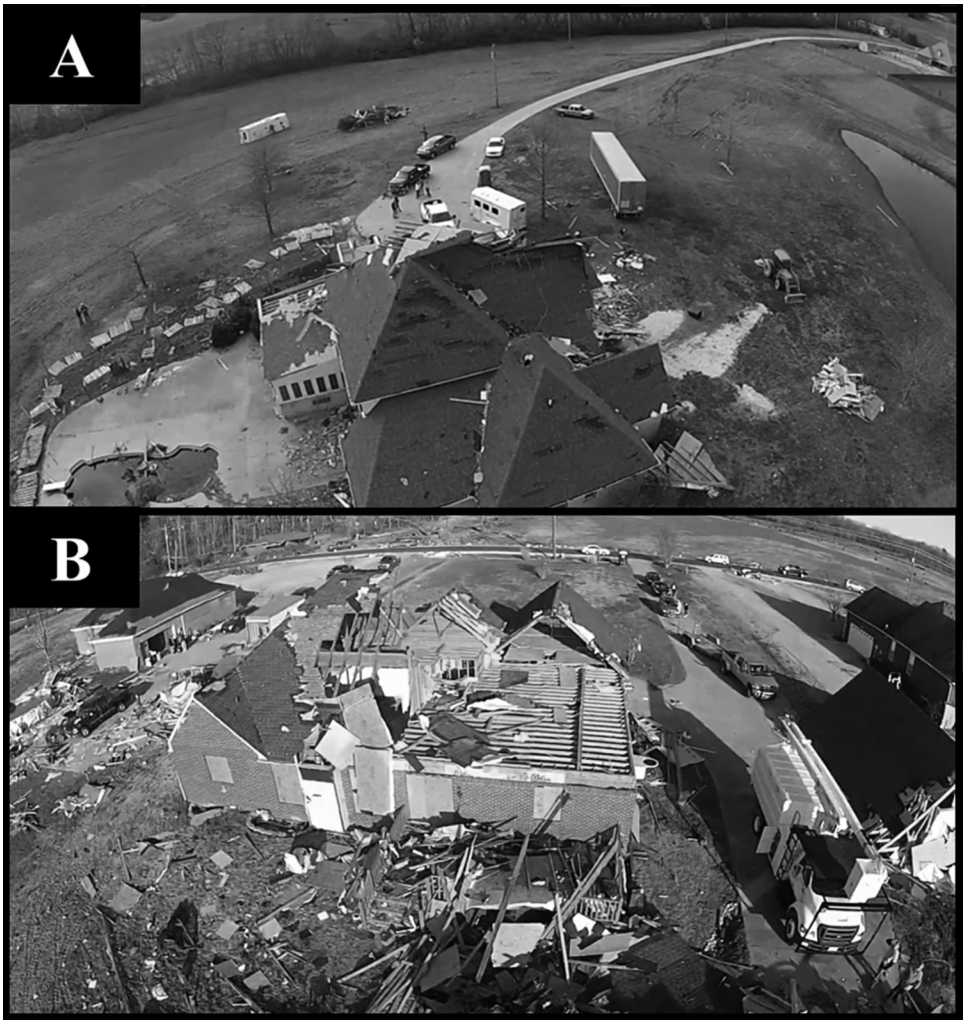

Figure 8. Sample UAS-based stills from video imagery of (A) Structure 1, and (B) Structure 2 showing oblique views of the damaged structures. The stills provide a visualization of the structure that illustrates object heights in more readily understandable manner than typical nadir views. Surrounding terrain, buildings, and infrastructure are also visible.

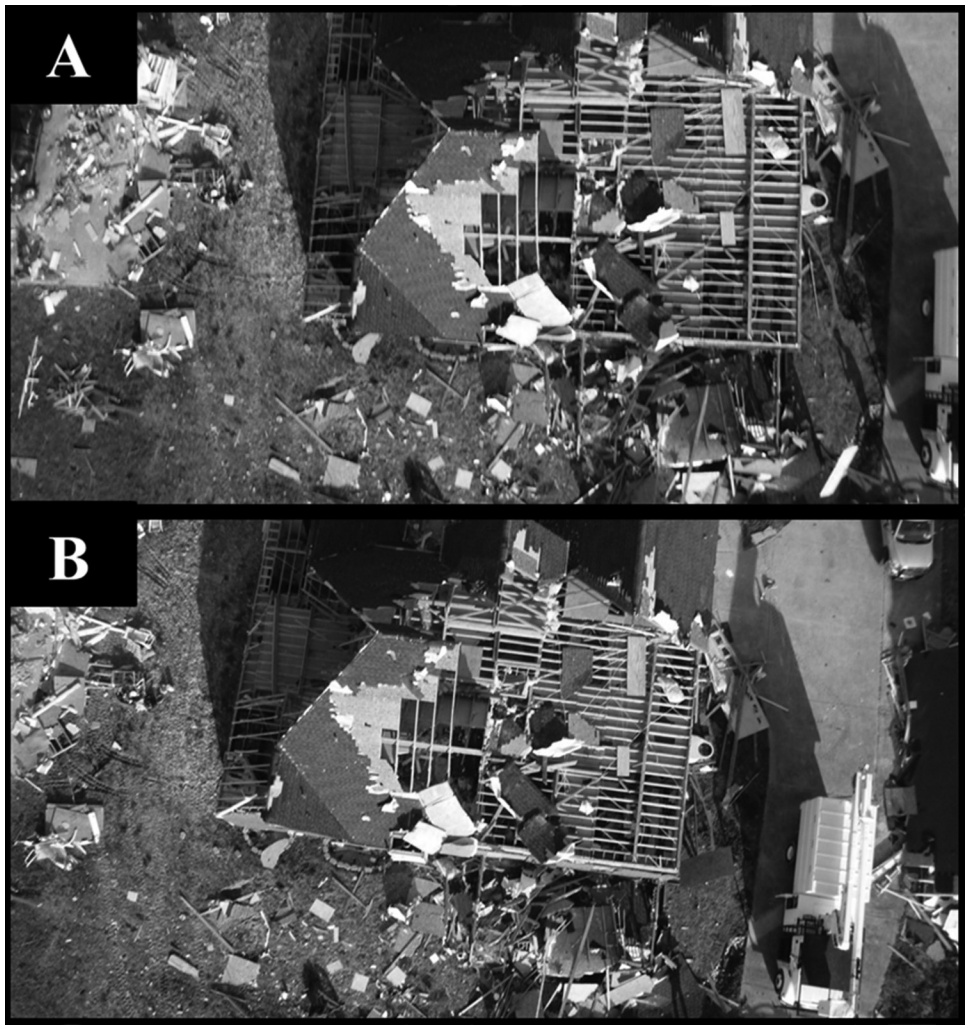

Figure 9. Two overlapping nadir images of Structure 2, potentially useable for stereo-photogrammetric analysis to estimate three-dimensional coordinates of different points on the building.

from the UAV-mounted camera as it tracks around the structure (see flight paths from Figure 2) provides a holistic view of the damaged structure and its surroundings. Figure 8A shows a small water body, trees in the distance, and a lack of nearby structures. Figure 8B similarly indicates trees in the distance as well as adjacent homes. Information on the immediate surroundings and the wider neighborhood can be important to understanding the wind loads on a building (i.e., exposure conditions) and the windborne debris environment.

In addition to the significant opportunities for qualitative image analysis described previously, UAS-based imagery can potentially be used for quantitative analysis as well. Overlapping images such as those shown in Figure 9 can be used for stereo-photogrammetric analysis. The principal of metric photogrammetry states that stereographic photography, specifically photographs with at least a 60 percent overlap of distinguishable objects within each picture, can be used to quantify object parameters (Li *et al.*, 2010). In this case study, the UAS operator was instructed to fly a pattern conducive for such imagery acquisition. However, significant winds during the UAS flights hindered acquisition of images with optimal overlap. Utilizing a pre-defined flight plan as well as an automated flight and/or camera operation could aid in achieving optimal imagery overlaps.

Conclusions

This paper provides insight into the potential use of UAS platforms for post-disaster imagery acquisition. Descriptions from the literature identified the role of UAS in obtaining post-disaster data and images for the purpose of gaining more detailed information about earthquake, tsunami, fire, hurricane and typhoon events. A post-tornado case study using a small multi-rotor UAS with still and video cameras was presented. The GSD of imagery collected with this system was approximately 0.007 m, two orders of magnitude better than typical NOAA post-disaster aerial imagery, making it much more suitable for investigation of damage at the individual building and neighborhood scales. The high resolution of the UAS-based imagery allowed identification of specific building materials (e.g., OSB roof sheathing), and individual bricks were clearly visible. Use of readily available digital cameras with even higher resolutions than the 12 megapixel unit used in this system, combined with lower flight altitudes above ground level, could easily improve the GSD to approximately 0.002 m. Wind gusts as high as 14 m/s during the UAS flights provided challenges for manual operation of the UAS and image collection, particularly as related to capturing images with suitable overlap for stereo-photogrammetric analysis.

As costs for UAS and digital cameras continue to drop, UAS flight and flight control capabilities continue to improve, and

given the demonstrated utility of these platforms, their use in post-disaster data collection is very likely to expand in the near future. Evolving FAA regulations governing UAS operations will play an important part in the speed of adoption of this technology.

Acknowledgments

The authors would like to express their thanks to LSU Research Associate Eddie Weeks for his UAS fieldwork and hands on training. Additionally, the contributions and expertise of Mr. Clifford Mugnier and Dr. Frank Willis are greatly appreciated.

Disclaimer

Certain commercial entities, equipment, or materials may be identified in this document in order to describe an experimental procedure or concept adequately. Such identification is not intended to imply recommendation or endorsement by the National Institute of Standards and Technology, nor is it intended to imply that the entities, materials, or equipment are necessarily the best available for the purpose.

References

Ackerman, E., 2011. Japan Earthquake: Global Hawk UAV May Be Able to Peek Inside Damaged Reactors, *IEEE Spectrum*, URL: *http://spectrum.ieee.org/automaton/robotics/military-robots/global-hawk-uav-may-be-able-to-peek-inside-damaged-reactors* (last date accessed: 08 October 2014).

Adams, S., C. Friedland, and M. Levitan, 2010. Unmanned aerial vehicle data acquisition for damage assessment in hurricane events, *Proceedings of the 8th International Workshop on Remote Sensing for Disaster Management*, 30 September - 01 October 2010, Tokyo, Japan.

Cohen, J., 2007. Drone spy plane helps fight California fires, *Science*, 318(5851):727. Federal Aviation Administration (FAA), 2011. *Fact Sheet: Unmanned Aircraft Systems (UAS)*, US Department of Transportation, Federal Aviation Administration, Washington, D.C., URL: *http://www.faa.gov/news/fact_sheets/news_story.cfm?newsId=14153* (last date accessed: 08 October 2014).

Federal Aviation Administration (FAA), 2013. FAA opens the Artic to commercial small unmanned aircraft, US Department of Transportation, Federal Aviation Administration, Washington, District of Columbia, USA, URL: http*://www.faa.gov/news/updates/?newsId=73981* (last date accessed: 08 October 2014).

Fox News, 2013. California fire officials using drone to help fight monster Yosemite blaze, URL: *http://www.foxnews.com/us/2013/08/29/california-fire-officials-using-drone-to-help-fight-monster-yosemite-blaze/* (last date accessed: 08 October 2014).

Gerke, M., and N. Kerle, 2011. Automatic structural seismic damage assessment with airborne oblique Pictometry imagery, *Photogrammetric Engineering & Remote Sensing*, 77(9):885–898.

Google, 2012. Google Earth, version 6.2, URL: *http://www.google.com/earth/index.html* (last date accessed: 08 October 2014).

Huber, M., 2010. Evergreen supports UAV team mapping Haitian Relief, Aviation International News, URL: *http://www.ainonline.com/aviation-news/aviation-international-news/2010-02-18/evergreen-supports-uav-team-mapping-haitian-relief* (last date accessed: 08 October 2014).

Li, C., L. Shen, H. Wang, and T. Lei, 2010. The research on unmanned aerial vehicle remote sensing and its applications, *Proceedings of the 2nd International Conference on Advanced Computer Control (ICACC)*, 27-29 March, Shenyang, Liaoning, China (International Association of Computer Science and Information Technology, Singapore), pp. 644-647.

Murphy, R., 2011. Have Robots been used in Previous Earthquakes?, Center for Robot-Assisted Search and Rescue, Texas Agricultural and Mechanical University, URL: *http://crasar.org/2011/03/13/have-robots-been-used-in-previous-earthquakes/* (last date accessed: 08 October 2014).

Murphy, R., 2012. A decade of rescue robots, *Proceedings of the International Conference on Intelligent Robots and Systems*, 07-12 October, Vilamoura, Algarve, Portugal (Institute of Electrical and Electronics Engineers/Robotics Society of Japan), pp. 5448–5549.

National Oceanic and Atmospheric Administration (NOAA), 2008. Remote Sensing Division: Hurricane Ike Base Map, URL: *http://ngs.woc.noaa.gov/ike/IKE0000.HTM* (last date accessed: 08 October 2014).

National Oceanic and Atmospheric Administration (NOAA), 2012. National Weather Service Weather Forecast Office: March 2nd, 2012 Storm Surveys for Alabama - Madison & Limestone Counties, URL: *http://www.srh.noaa.gov/hun/?n=03022012_limes_mad_ef3* (last date accessed: 08 October 2014).

Nebiker, S., A. Annen, M. Scherrer, and D. Oesch, 2008. A light-weight multispectral sensor for micro UAV - Opportunities for very high resolution airborne remote sensing, *The International Archives of the Photogrammetry, Remote Sensing and Spatial Information Sciences*, 37:1193–1200.

Pratt, K., R.R. Murphy, S. Stover, and C. Griffin, 2006. Requirements for semi-autonomous flight in miniature UAVs for structural inspection, *Proceedings of the AUVSI's Unmanned Systems North American Conference*, 29-31 August, Orlando, Florida (Association for Unmanned Vehicle Systems International, Arlington, Virginia).

Quaritsch, M., K. Kruggl, D. Wischounig-Strucl, M. Shah, and B. Rinner, 2010. Networked UAVs as aerial sensor network for disaster management applications, *Elektrotechnik und Informationstechnik - Special Issue on Wireless Sensor Networks*, 127(3):56–63.

Reavis, B., and B. Hem, 2011. Honeywell T-Hawk Aids Fukushima Daiichi Disaster Recovery: Unmanned Micro Air Vehicle Provides Video Feed to Remote Monitors, Honeywell Aerospace Media Center, Honeywell International Inc., URL: *http://honeywell.com/News/Pages/Honeywell-T-Hawk-Aids-Fukushima-Daiichi-Disaster-Recovery.aspx* (last date accessed: 08 October 2014).

Steimle, E.T., R.R. Murphy, M. Lindemuth, and M.L. Hall, 2009. Unmanned marine vehicle use at Hurricanes Wilma and Ike, *Proceedings of the OCEANS 2009 - Marine Technology for Our Future: Global and Local Challenges*, 26-29 October, Biloxi, Mississippi (Marine Technology Society/Institute of Electrical and Electronics Engineers), pp. 1–6.

Vincenzi, D., D.C. Ison, and B.A. Terwilliger, 2014. The role of unmanned aircraft systems (UAS) in disaster response and recovery efforts: historical, current, and future, *Proceedings of the Unmanned Systems 2014*, 13-15 May, Orlando, Florida (Association for Unmanned Vehicle Systems International).

VT Group, 2011. Devastating Earthquake in Haiti: Pioneering Technology Application Save Time & Resources, VT Group Portland, Oregon, URL: *www.vt-group.com/unmanned* (last date accessed: 08 October 2014).